

How much entanglement is needed for emergent anyons and fermions?

Zhi Li,¹ Dongjin Lee,^{1,2} and Beni Yoshida¹

¹*Perimeter Institute for Theoretical Physics, Waterloo, Ontario N2L 2Y5, Canada*

²*Department of Physics and Astronomy, University of Waterloo, Waterloo, Ontario N2L 3G1, Canada*

It is known that particles with exotic properties can emerge in systems made of simple constituents such as qubits, due to long-range quantum entanglement. In this paper, we provide quantitative characterizations of entanglement necessary for emergent anyons and fermions by using the geometric entanglement measure (GEM) which quantifies the maximal overlap between a given state and any short-range entangled states. For systems with emergent anyons, based on the braiding statistics, we show that the GEM scales linearly in the system size regardless of microscopic details. The phenomenon of emergent anyons can also be understood within the framework of quantum error correction (QEC). Specifically, we show that the GEM of any 2D stabilizer codes must be at least quadratic in the code distance. Our proof is based on a generic prescription for constructing string operators, establishing a rigorous and direct connection between emergent anyons and QEC. For systems with emergent fermions, despite that the ground state subspaces could be exponentially huge and their coding properties could be rather poor, we show that the GEM also scales linearly in the system size. Our results also establish an intriguing link between quantum anomaly and entanglement: a quantum state respecting anomalous 1-form symmetries, be it pure or mixed, must be long-range entangled, offering a non-trivial class of intrinsically mixed state phases.

I. INTRODUCTION

Quantum information processing is intrinsically vulnerable to noises and decoherence that may arise from physical interactions with the environment as well as engineering imperfections in handling qubits. A useful way to fault-tolerantly store and process quantum information is to utilize particles with exotic statistical properties known as anyons which provide ideal platforms with naturally arising topological protection from otherwise detrimental errors [1, 2]. While anyons do not naturally exist as elementary particles in our universe, they do *emerge* as low-energy excitations in strongly correlated many-body quantum systems. Theoretical and experimental search of anyons remains one of the most active areas of research in modern physics.

The emergent phenomenon of anyons is closely related to long-range entanglement in many-body systems [3–8]. A vivid feature of quantum entanglement is the superposition: construction of wavefunctions requires a large number of product basis states. For instance, consider a ground state of the 2D toric code. It can be expressed as a sum of exponentially many computational (Z -basis) states

$$|\Psi_{\text{toric}}\rangle = \frac{1}{\sqrt{2^{n/2}}} \prod_{\text{vertex}} (I + X \begin{array}{c} \times \\ \times \\ \times \end{array} X) |0\rangle^n \propto \sum_{\alpha \in \text{closed-loop}} |\alpha\rangle \quad (1)$$

where each term can be viewed as a closed loop configuration by drawing a line connecting qubits in $|1\rangle$. This characterization of the toric code is an example of the string-net condensation picture which hosts a wide generalization for non-chiral topological order [9]. Anyonic excitations can be generally created at endpoints of an open string operator γ applied to the entangled ground

state. Non-trivial braiding statistics of anyons imply that the ground state cannot be prepared by a short-depth quantum circuit, and thus must be long-range entangled [3, 10, 11].

The degree of superpositions in a given wavefunction $|\Psi\rangle$ can be quantitatively measured by the Geometric Entanglement Measure (GEM) of the form [12–17]

$$E(\Psi) = - \max_{|P\rangle : \text{product}} \log_2 |\langle \Psi | P \rangle|^2 \quad (2)$$

which computes the maximum overlap between $|\Psi\rangle$ and product states. Unfortunately, this measure fails to distinguish short-range and long-range entanglement, since short-range entangled states, such as the cluster state, can score high on the GEM. To circumvent this problem, the depth- t Geometric Entanglement Measure (depth- t GEM) was proposed [18]

$$E_t(\Psi) = - \max_{U : \text{depth}(U)=t} \log_2 |\langle \Psi | U | 0^n \rangle|^2 \quad (3)$$

which considers the maximum overlap between $|\Psi\rangle$ and all short-range entangled states $U|0\rangle^n$. Here, the maximum is taken over all n -qubit geometrically local (e.g., brickwall) depth- t quantum circuits; a depth-0 circuit is defined as a product of single-qubit gates, and hence $E(\Psi) = E_0(\Psi)$.

This generalization of GEM provides a refined characterization of long-range entanglement. According to the conventional definition, a quantum state $|\Psi\rangle$ is said to be long-range entangled if it cannot be (approximately) prepared by a short-depth circuit. In terms of the GEM, this simply amounts to $E_t(\Psi) \neq 0$ (or $E_t(\Psi) > \epsilon$ if approximations are accounted) for small t . However, depending on its underlying entanglement structure, each long-range entangled state $|\Psi\rangle$ can have strikingly different values of $E_t(\Psi)$. Some long-range entangled states score very low on the GEM, suggesting that they have a

significant overlap with short-range entangled states despite their high quantum circuit complexity. On the contrary, genuinely long-range entangled states score very high on the GEM, suggesting that they not only cannot be approximated by short-range entangled states, but also must be almost orthogonal to any short-range entangled states. For instance, the GHZ state $\frac{1}{\sqrt{2}}(|0\rangle^n + |1\rangle^n)$ is long-range entangled since it cannot be prepared from a product state by a constant depth circuit. However, the GHZ state scores small for depth- t GEM, namely $E_t(\text{GHZ}) \sim O(1)$ for any $t \sim O(1)$. This aligns with our intuition concerning the intrinsic instability of entanglement in the GHZ state. On the other hand, as we will prove later in this paper, the toric code has $E_t(\text{toric}) \sim O(n)$ for $t \sim O(1)$, reflecting its complex entanglement structure.

In this work, we use the depth- t GEM as a more direct, quantitative characterization of quantum entanglement that is needed for emergent anyons and other exotic physical objects.

Emergent anyons

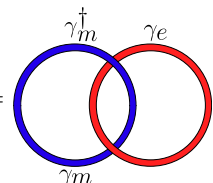
In this paper, we begin by studying two-dimensional spin systems whose ground states support anyonic excitations with non-trivial braiding statistics. While we focus on the toric code for simplicity of presentation, similar results can be generically derived.

Result 1. A ground state $|\Psi\rangle$ of the toric code satisfies

$$E_t(\Psi) = \Omega(n), \quad (4)$$

where the multiplicative coefficient only depends on t .

The proof involves several steps, but the underlying physical picture is simple enough to summarize here. Recall that the toric code supports two types of abelian anyonic excitations, e and m , that can be created at endpoints of string-like operators. Such operators can be deformed while fixing the endpoints and create the same sets of anyons. The braiding statistics between e and m can be probed by considering a pair of closed and open string operators as follows

$$\langle \Psi | \gamma_m^\dagger \gamma_e \gamma_m | \Psi \rangle = \langle \Psi | \gamma_m^\dagger \gamma_e \gamma_m | \Psi \rangle = -1. \quad (5)$$


The key observation is that due to the deformability of γ_m string, the region that supports the pair of m anyons must be decoupled from the rest of the system if $|\Psi\rangle$ was short-range entangled, so that the γ_e loop “does not know” whether there were or were not an m anyon inside. Therefore, $\langle \Psi | \gamma_m^\dagger \gamma_e \gamma_m | \Psi \rangle = 1$. This contradicts

the braiding statistics, which proves that the toric code ground states must be long-range entangled. The above beautiful argument is due to Bravyi (unpublished) and was described in [11].

To prove the claimed linear lower bound on $E_t(\Psi)$, we consider $O(n)$ copies of braiding processes in non-overlapping subregions where each process contributes $O(1)$ to $E_t(\Psi)$. This argument can be readily extended to ground states of any spin systems that support non-trivial anyonic excitations. Namely, we can show that the non-trivial braiding $\langle \gamma_a^\dagger \gamma_b \gamma_a \rangle \neq 1$ for two anyons a, b is inconsistent with short-range entanglement, and as such, a similar lower bound on $E_t(\Psi)$ follows.

Emergent fermions

Next, we will turn our attention to systems that support emergent fermions. To be concrete, we will focus on the following variant of the Kitaev honeycomb model [19]:

$$H_{\text{fermion}} = - \sum_{\square} S_{\square}, \quad S_{\square} = X \begin{array}{c} Y \quad Z \\ \diagdown \quad \diagup \\ \square \\ \diagup \quad \diagdown \\ Z \quad Y \end{array} X. \quad (6)$$

Viewed as a stabilizer code, a ground state satisfies $S_{\square}|\Psi\rangle = +|\Psi\rangle$, and the code parameters are $k \sim n/2$ and $d = 2$. Despite the exponentially large code subspace 2^k and the small code distance d , a linear lower bound, which is applicable to *arbitrary* ground state, can be proven.

Result 2. A ground state $|\Psi\rangle$ of the honeycomb model satisfies

$$E_t(\Psi) = \Omega(n), \quad (7)$$

where the multiplicative coefficient only depends on t .

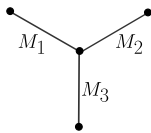
Unlike anyons in the toric code, fermions have trivial braiding statistics (i.e., they are not anyons). Hence, our proof utilizes the fermion exchange statistic crucially. Before proceeding, however, it is worth emphasizing an important difference between how anyons and fermions emerge in the toric code and the honeycomb model respectively. In the toric code, anyons emerge as low-energy excitations *outside* the energy ground space. On the contrary, in the honeycomb model, fermions emerge *inside* the ground energy subspace. Recall that the honeycomb model possesses the following two-body logical operators

$$X \text{---} X \quad Y \text{---} Y \quad Z \text{---} Z \quad (8)$$


that commute with stabilizers S_{\square} . Let us pick an arbitrary ground state $|\Psi\rangle$ and regard it as a “vacuum”

state with no fermions. Consider an open string operator M which is generated from two-body logical operators. Then, $M|\Psi\rangle$ can be interpreted as a state with two emergent fermions at endpoints of an open string M . The crucial point is that $M|\Psi\rangle$ still lives in the energy ground space as M is a logical operator of the code.

The particle exchange statistics can be probed by considering three string-like operators M_1, M_2, M_3 that share a common endpoint [20]:



$$M_3 M_2 M_1 |\Psi\rangle = e^{i\theta} M_1 M_2 M_3 |\Psi\rangle, \quad (9)$$

where $e^{i\theta} = -1$ for fermions. In the honeycomb model, this relation can be explicitly verified as three string-like logical operators anti-commute with each other at the overlapping qubit. Using a variant of Bravyi's idea, it can be shown that short-range entanglement and the deformability of string-like operators would imply $\langle\Psi| M_3^\dagger M_2^\dagger M_1^\dagger M_3 M_2 M_1 |\Psi\rangle = 1$, contradicting with the exchange statistics. Then, with some extra work, the claimed linear lower bound on $E_t(\Psi)$ can be obtained.

Mixed state and Anomalous symmetry

The aforementioned result on emergent fermions has interesting implications from the perspectives of mixed states and anomalous symmetries.

Mixed states: Characterization of quantum entanglement for mixed states is a considerably harder question compared to its counterpart for pure states. Quantum circuit complexity of preparing a mixed state has been studied in quantum information theory in the context of topological quantum memory at finite temperature [2, 21]. Recently, there has been renewed interest in the possibility of novel quantum phases, that are genuinely intrinsic to mixed state, in the condensed matter community. Generally, a mixed state ρ is said to be short-range entangled if ρ can be expressed as a probabilistic ensemble of short-range entangled states [21]:

$$\rho = \sum_j p_j |\psi_j\rangle\langle\psi_j|, \quad |\psi_j\rangle = U_j |0\rangle^n, \quad (10)$$

where U_j are short-depth circuits. A naturally arising question is whether a mixed state ρ in the ground state space of the honeycomb model is long-range entangled or not. Evidence for long-range entanglement in ρ was reported in [22] where a subleading contribution in the entanglement negativity, similar to topological entanglement entropy, was found. Here, as a simple corollary of the aforementioned result, we can prove that ρ in the honeycomb model is indeed long-range entangled.

Result 2' (Mixed state). Any mixed state ρ satisfying the hexagonal constraints $\text{Tr}(\rho S_\square) = 1$ in the honeycomb

model cannot be written as an ensemble of short-range entangled states.

Anomalous symmetries: Recently, there has been considerable progress in understanding the relation between quantum entanglement and anomalous symmetries. To motivate this viewpoint, consider a system with conventional symmetries, such as a \mathbb{Z}_2 global symmetry generated by $S = \otimes_{j=1}^n X_j$. The system is equipped with well-defined local \mathbb{Z}_2 charge generators which are simply X_j 's. The symmetry constraint of the form $S|\Psi\rangle = |\Psi\rangle$ then dictates that the total \mathbb{Z}_2 charge in $|\Psi\rangle$, expressed as a product of local \mathbb{Z}_2 generators X_j , must be trivial (+1). Furthermore, the system has a natural "vacuum" state, namely $|+\rangle^n$ for which local generators X_j act trivially, and thus is not entangled.

On the contrary, anomalous symmetries do not admit locally definable charge generators. A prototypical example of this phenomenon is a 1D \mathbb{Z}_2 anomalous global symmetry, often called the CZX symmetry S_{CZX} [23], which is generated by

$$S_{CZX} = S_{CZ} S_X, \quad (11)$$

where $S_{CZ} = \prod_j CZ_{j,j+1}$, $S_X = \prod_j X_j$. This operator defines a global \mathbb{Z}_2 symmetry as $S_{CZX}^2 = I$ (for even n), but does not possess local generators. For instance, one might want to consider $CZ_{j,j+1} X_j$ as a local generator. Unfortunately, a product of $CZ_{j,j+1} X_j$ does not generate $S_{CZX} = S_{CZ} S_X$. Furthermore, $CZ_{j,j+1} X_j$ does not commute with S_{CZX} , and also they do not commute with each other. As such, consistent meaning as local charge generators cannot be given to them.

This impossibility of decomposing an anomalous symmetry operator into local charge generators is closely related to quantum entanglement. This viewpoint has been extensively studied from the perspective of symmetry-protected topological (SPT) order, as the CZX symmetry emerges at the boundary of a 2D \mathbb{Z}_2 SPT phase [23]. Recently, it has been rigorously shown that any wavefunctions satisfying $S_{CZX}|\Psi\rangle = |\Psi\rangle$ must be multipartite entangled [24].

Returning to the honeycomb model, the upshot is that the hexagonal stabilizers S_\square are another example of anomalous symmetries. More precisely, these are 1-form anomalous symmetries since S_\square acts as a codimension-1 operator instead of a global codimension-0 operator as in the CZX model. The anomalous nature of S_\square symmetries can be seen from the fact that they cannot be cut into two pieces. For example, suppose we cut S_\square vertically into two parts and write it as a product of the left and right parts, $S_\square = S_\square^{(L)} S_\square^{(R)}$. We immediately notice that $S_\square^{(L)}$ and $S_\square^{(R)}$ do not commute with S_\square , and thus are not well defined as local generators. Instead, one might decompose S_\square as a product of two-body logical operators from Eq. (8). While this decomposition consists of operators that commute with S_\square symmetries, two-body operators anti-commute with each other, and hence do not admit interpretations as local generators.

Our result on the honeycomb model can be rephrased as follows.

Result 2'' (Anomalous symmetry). Any state $|\Psi\rangle$ satisfying anomalous 1-form symmetries $S_{\square}|\Psi\rangle = |\Psi\rangle$ in the honeycomb model must be long-range entangled. Furthermore they satisfies $E_t(\Psi) = \Omega(n)$.

While wavefunctions with anomalous global symmetries are long-range entangled in general, they may score very low in terms of the GEM. For instance, the GHZ state $\frac{1}{\sqrt{2}}(|0\rangle^n + |1\rangle^n)$ satisfies the CZX symmetry, but it has $E_0(\text{GHZ}) = 1$. This is in contrast with anomalous 1-form symmetries, such as S_{\square} symmetries, where the GEM scales linearly with respect to n .

2D stabilizer codes

The phenomenon of emergent anyons can be understood within the framework of quantum error correction (QEC) where quantum information is stored in the energy ground state space. This motivates us to ask whether there is a fundamental lower bound on the necessary quantum entanglement for storing quantum information in a bounded volume of space.

In this paper, we reveal a universal lower bound on $E_t(\Psi)$ for certain two-dimensional QEC systems. Specifically, we will consider a system of n qubits placed on a 2D lattice and focus on codes for which the code subspace \mathcal{C} is defined by geometrically local stabilizer generators S_j : the code subspace \mathcal{C} can be realized as the energy ground subspace of a local gapped Hamiltonian

$$H = - \sum_j S_j. \quad (12)$$

The QEC capability is usually measured by its code distance. A code is said to have code distance d if logical states are locally indistinguishable on any subset of less than d physical qubits.

Our main result is the following lower bound on the GEM.

Result 3. For a 2D geometrically local stabilizer code, if the code distance $d > d_0$, then any logical state $|\Psi\rangle$ satisfies

$$E_t(\Psi) = \Omega(d^2). \quad (13)$$

Here, both the multiplicative constant and d_0 depend only on t and the size of stabilizer generators.

For the toric code, $d = \Theta(\sqrt{n})$, hence result 3 is in accordance with Result 1. There is, however, a crucial difference. The starting point of Result 1 is the emergent anyons, which exist on any geometries including the sphere. The starting point of Result 3, on the other hand, is the QEC property which relies on the ground state degeneracy. Therefore, Result 3 does not apply to the toric code on the sphere per se.

Nevertheless, the proof of result 3 reflects a rigorous and direct connection between QEC and emergent anyons. The main idea is that we can derive the existence of emergent anyons *solely* based on the error correction property. More precisely, as long as the code distance d is sufficiently larger than the size of local stabilizer generators, we can always construct loop-like operators γ_b that only create syndrome at endpoints, as well as string-like stabilizer operators γ_a , such that $\langle \gamma_a^\dagger \gamma_b \gamma_a \rangle = -1$. Key technical tools in the constructions of loop and string-like operators are the cleaning lemma [25] and the disentangling lemma [26] which allows us to identify a pair of anti-commuting logical operators. Specifically, these logical operators can be designed to be supported on unions of line-like subregions. We then introduce a simple but powerful truncation procedure of stabilizer operators which enables us to obtain the braiding configuration similar to Eq. (5). Such braiding statistics are not compatible with short-range entanglement, which ultimately leads to the desired linear lower bound on the GEM.

The anyon braiding statistics then simply follow by interpreting the syndromes at the end of string operators as anyons. From this point of view, our result implies that anyons always emerge from QEC in 2D stabilizer codes, namely, from the sole assumption of the code distance.

Relation to previous work

In the previous work, we derived generic lower bounds on depth- t GEM for QEC codes in several settings [18]. The most relevant to the present paper is the following universal lower bound for a quantum Low-Density Parity-Check (LDPC) code with the code distance d :

$$E_t(\Psi) = \Omega(d), \quad (14)$$

where the multiplicative coefficient depends only on the sparsity of the qLDPC code and the depth t . The linear scaling with d cannot be improved further as there exist qLDPC codes with the distance $d \sim n$. This lower bound, however, is not tight for quantum codes supported on lattices with geometrically local projectors. For instance, the two-dimensional toric code has $E_0(\Psi) \sim n/2$, but its code distance is $d \sim \sqrt{n}$. Also, the above lower bound is not applicable to the toric ‘‘code’’ without logical qubits (e.g., supported on a sphere) as its derivation crucially depends on the presence of logical qubits. Finally, the above bound is not particularly useful in studying long-range entanglement in the honeycomb model as its code distance is $d = 2$.

Our results in the present work improve the above qLDPC lower bound in various ways by focusing on two-dimensional systems. Result 1 proves that the quadratic scaling $E_t(\text{toric}) = \Omega(d^2)$ ($t \sim O(1)$) for the toric code. Result 3 further improves this characterization for the cases of 2D local stabilizer codes by proving $E_t(\Psi) = \Omega(d^2)$. Result 2 proves that, despite the poor coding

properties, all the codeword states in the honeycomb model are long-range entangled with $E_t(\Psi) = \Omega(n)$.

Plan of the paper

This paper is organized as follows. In section II, we study the toric code as a prototypical example of systems with emergent anyons. In section III, we will derive a generic lower bound on the GEM for arbitrary 2D local stabilizer codes. In section IV, we will study the honeycomb model and show that wavefunctions with anomalous 1-form symmetries have $E_t(\Psi) = \Omega(n)$. In section V, we conclude with brief discussions.

II. 2D TORIC CODE

We will prove the following linear lower bound on $E_t(\Psi)$ for a toric code ground state.

Theorem 1. Given a toric code ground state $|\Psi\rangle$, there exists $\alpha > 0$ such that if $t \leq O(\sqrt{n})$, then

$$E_t(\Psi) > \frac{\alpha n}{(t+1)^2}. \quad (15)$$

A. Anyon braiding statistics

Recall that the toric code Hamiltonian is given by

$$H_{\text{toric}} = - \sum_{+} A_{+} - \sum_{\square} B_{\square}, \quad (16)$$

where $A_{+} = \prod_{j \in +} X_j$ and $B_{\square} = \prod_{j \in \square} Z_j$. Qubits reside on edge of an $L \times L$ square lattice, and $+$ (\square) denote vertices (plaquettes). A ground state $|\Psi\rangle$ satisfies $A_{+}|\Psi\rangle = B_{\square}|\Psi\rangle = |\Psi\rangle$.

Microscopic details of the construction, however, are not important. A crucial property we use for the proof is the non-trivial braiding statistics of anyons of the toric code. Namely, consider a pair of a closed string operator γ_e and an open string operator γ_m which consist of Pauli Z and X operators respectively (Fig. 1). Considering a process of braiding e around m , we find

$$\gamma_m \gamma_e \gamma_m |\Psi\rangle = -|\Psi\rangle. \quad (17)$$

This braiding statistics is stable under deformation by a constant depth circuit U_t . Namely, for a deformed toric code ground state $|\Psi_t\rangle \equiv U_t|\Psi\rangle$, define dressed string operators by $\tilde{\gamma}_m = U_t \gamma_m U_t^\dagger$, $\tilde{\gamma}_e = U_t \gamma_e U_t^\dagger$. Eq. (17) still holds for $|\Psi_t\rangle$ and $\tilde{\gamma}_m, \tilde{\gamma}_e$, but dressed string operators $\tilde{\gamma}_m, \tilde{\gamma}_e$ now have width $O(t)$. One can then consider a quasi-local anyon braiding process as in Fig. 1 by taking a larger region of linear size t .

B. Long-range entanglement

We first prove that a toric code ground state is long-range entangled.

Lemma 1. Given a toric code ground state $|\Psi\rangle$, we have

$$U_t|\Psi\rangle \neq |0^n\rangle \quad (18)$$

for any depth- t unitary U_t with constant t .

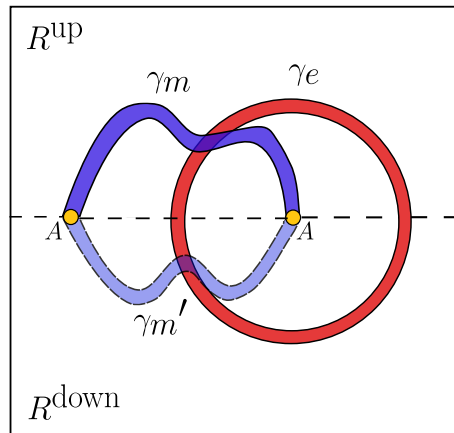


FIG. 1. Two dressed anti-commuting string operators for anyon braiding in a deformed toric code. Their width is at most $2t$. For the purpose of the proof, it suffices to consider a region R with a linear size of $8t$.

Proof. The proof is similar to Bravyi's proof described in Ref. [11]. Suppose that the Eq. (18) is false. In terms of a deformed state $|\Psi_t\rangle \equiv U_t|\Psi\rangle$, this is equivalent to $|\Psi_t\rangle = |0^n\rangle$. Since U_t is a finite depth circuit, the braiding process of Eq. (17) can be considered by a pair of dressed string operators $\tilde{\gamma}_m = U_t \gamma_m U_t^\dagger$ and $\tilde{\gamma}_e = U_t \gamma_e U_t^\dagger$. Below, we will omit the tilde and represent dressed operators by γ_m, γ_e in order to avoid cluttering in equations.

As in Fig. 1, we use a dressed string operator γ_m to create two m anyons supported on region A . We claim that

$$\gamma_m |\Psi_t\rangle = |\phi_A\rangle \otimes |0_{A^c}\rangle, \quad (19)$$

where $|\phi_A\rangle$ is a state in the Hilbert space \mathcal{H}_A , $|0_{A^c}\rangle$ is the product state of $|0\rangle$ for all qubits outside A . To show this, we divide the system into three subregions: A , R^{up} and R^{down} as in Fig. 1. We can find another string operator γ'_m that is supported on $A \cup R^{\text{down}}$ satisfying

$$\gamma'_m |\Psi_t\rangle = \gamma_m |\Psi_t\rangle. \quad (20)$$

Define Π^{up} as an operator that projects $\mathcal{H}_{R^{\text{up}}}$ to $|0_{R^{\text{up}}}\rangle$. We have, by assuming Eq.(18) is false,

$$\begin{aligned} \Pi^{\text{up}} \gamma'_m |\Psi_t\rangle &= \gamma'_m \Pi^{\text{up}} |\Psi_t\rangle = \gamma'_m \Pi^{\text{up}} |0^n\rangle \\ &= \gamma'_m |0^n\rangle = \gamma'_m |\Psi_t\rangle. \end{aligned} \quad (21)$$

Similarly,

$$\Pi^{\text{down}} \gamma_m |\Psi_t\rangle = \gamma_m |\Psi_t\rangle. \quad (22)$$

Combining the above three equations, we have

$$\Pi^{\text{up}} \Pi^{\text{down}} \gamma_m |\Psi_t\rangle = \gamma_m |\Psi_t\rangle, \quad (23)$$

and hence Eq. (19) is proved.

Now we apply a loop operator γ_e on $\gamma_m |\Psi\rangle$. Recall that γ_e is a deformed stabilizer, and hence $\gamma_e |\Psi_t\rangle = |\Psi_t\rangle$. Assuming Eq.(18) is false, this implies $\gamma_e |0_{A^c}\rangle = |0_{A^c}\rangle$. Therefore, due to Eq. (19), we have

$$\begin{aligned} \gamma_e \gamma_m |\Psi_t\rangle &= |\phi_A\rangle \otimes \gamma_e |0_{A^c}\rangle = |\phi_A\rangle \otimes |0_{A^c}\rangle \\ &= \gamma_m |\Psi_t\rangle. \end{aligned} \quad (24)$$

This, however, contradicts Eq. (17), namely $\gamma_m \gamma_e \gamma_m |\Psi_t\rangle = -|\Psi_t\rangle$, which completes the proof. \square

It is worth mentioning that the proof based on the Lieb-Robinson bound in Ref. [3] crucially uses the ground state degeneracy while the above proof (based on Ref. [11]) applies to the toric code with no ground state degeneracy as well.

C. Overlap with short-range entangled state

The result of the above lemma is equivalent to $E_t(\Psi) > 0$, and is in general not sufficient to obtain a lower bound for $E_t(\Psi)$ that would scale with the system size.

We now prove an upper bound on the maximum overlap between ρ_R of a deformed toric code ground state and $|0_R\rangle$ for a patch R of linear size t .

Lemma 2. Let R be any patch of linear size $8(t+1)$. Given a deformed toric code ground state $|\Psi_t\rangle = U_t |\Psi\rangle$ with a depth t circuit U_t , there exists a constant $\epsilon > 0$ such that, in terms of trace norm,

$$\|\rho_R - |0_R\rangle\langle 0_R|\|_1 > \epsilon, \quad (25)$$

where $\rho_R = \text{Tr}_{R^c}(|\Psi_t\rangle\langle\Psi_t|)$, and accordingly,

$$\mathcal{F}(|0_R\rangle, \rho_R) < 1 - \frac{1}{4}\epsilon^2 = 1 - \epsilon' \quad (26)$$

for some $\epsilon' > 0$.

Proof. Let γ_m and γ_e be dressed string operators. Suppose that the Eq. (25) is false. We claim that

$$\gamma_m |0_R\rangle\langle 0_R| \gamma_m^\dagger \approx |0_{A^c}\rangle\langle 0_{A^c}| \otimes \rho'_A, \quad (27)$$

where \approx means that the trace distance is smaller than a constant $O(\epsilon)$. Here A^c refers to the complement of A inside the patch R .

The proof is a more quantitative version of lemma 1. We have

$$\Pi^{\text{up}}(\gamma_m |0_R\rangle\langle 0_R| \gamma_m^\dagger) \Pi^{\text{up}}$$

$$\begin{aligned} &\approx \Pi^{\text{up}}(\gamma_m \rho_R \gamma_m^\dagger) \Pi^{\text{up}} \\ &= \Pi^{\text{up}}(\gamma_{m'} \rho_R \gamma_{m'}^\dagger) \Pi^{\text{up}} = \gamma_{m'} (\Pi^{\text{up}} \rho_R \Pi^{\text{up}}) \gamma_{m'}^\dagger \\ &\approx \gamma_{m'} (\Pi^{\text{up}} |0_R\rangle\langle 0_R| \Pi^{\text{up}}) \gamma_{m'}^\dagger = \gamma_{m'} (|0_R\rangle\langle 0_R|) \gamma_{m'}^\dagger \\ &\approx \gamma_{m'} \rho_R \gamma_{m'}^\dagger = \gamma_m \rho_R \gamma_m^\dagger \\ &\approx \gamma_m |0_R\rangle\langle 0_R| \gamma_m^\dagger, \end{aligned} \quad (28)$$

and

$$\begin{aligned} &\Pi^{\text{down}}(\gamma_m |0_R\rangle\langle 0_R| \gamma_m^\dagger) \Pi^{\text{down}} \\ &= \gamma_m \Pi^{\text{down}} |0_R\rangle\langle 0_R| \Pi^{\text{down}} \gamma_m^\dagger = \gamma_m |0_R\rangle\langle 0_R| \gamma_m^\dagger. \end{aligned} \quad (29)$$

Therefore,

$$\begin{aligned} \gamma_m |0_R\rangle\langle 0_R| \gamma_m^\dagger &\approx \Pi^{\text{down}} \Pi^{\text{up}}(\gamma_m |0_R\rangle\langle 0_R| \gamma_m^\dagger) \Pi^{\text{up}} \Pi^{\text{down}} \\ &= |0_{A^c}\rangle\langle 0_{A^c}| \otimes \rho'_A. \end{aligned} \quad (30)$$

Using this approximation, we obtain

$$\begin{aligned} &\text{Tr}(\gamma_e \gamma_m \rho_R \gamma_m^\dagger) \\ &\approx \text{Tr}(\gamma_e \gamma_m |0_R\rangle\langle 0_R| \gamma_m^\dagger) \\ &\approx \text{Tr}((\gamma_e |0_{A^c}\rangle\langle 0_{A^c}|) \otimes \rho'_A) = \text{Tr}(\gamma_e |0_{A^c}\rangle\langle 0_{A^c}|) \text{Tr}(\rho'_A) \\ &\approx \text{Tr}(\gamma_e |0_{A^c}\rangle\langle 0_{A^c}|) = \text{Tr}(\gamma_e |0_R\rangle\langle 0_R|) \\ &\approx \text{Tr}(\gamma_e \rho_R) = \langle \Psi_t | \gamma_e | \Psi_t \rangle = 1 \end{aligned} \quad (31)$$

which contradicts Eq. (17). \square

Finally, to complete the proof of Thm. 1, we divide the whole system into multiple regions R_i such that mutual distances are larger than $2t$. For a (deformed) toric code, we have the following decoupling property:

$$\rho_R = \otimes_i \rho_{R_i}, \quad R = \cup_i R_i \quad (32)$$

since stabilizer generators are geometrically local and each region R_i is correctable [27]. From this and the monotonicity of fidelity, we obtain

$$\begin{aligned} \mathcal{F}(|\Psi_t\rangle, |0_n\rangle) &\leq \mathcal{F}(\rho_R, |0_R\rangle) = \prod_i \mathcal{F}(\rho_{R_i}, |0_{R_i}\rangle) \\ &< (1 - \epsilon')^{\frac{c'n}{(t+1)^2}}, \end{aligned} \quad (33)$$

where $c'n/(t+1)^2$ is a number of disentangled patches. This proves theorem 1.

III. 2D LOCAL STABILIZER CODES

In the previous section, we derived the GEM lower bound for the toric code based on emergent anyons. The toric code model stands out as a quintessential example of topological quantum error-correcting codes. In this section, we show that a similar bound applies more broadly to all 2D geometrically local stabilizer codes with or without boundaries (the geometric locality here is defined using the standard Euclidean geometry).

Theorem 2. For 2D geometrically local stabilizer codes, denote w as the maximal diameter of stabilizer generators. If $d > \Theta((w+t)^2)$, we have:

$$E_t(\Psi) > \alpha \frac{d^2}{w^2(w+t)^2}. \quad (34)$$

for some $\alpha > 0$.

Although the starting point here is quantum error correction instead of anyons, our proof strategy is similar to the one for the toric code using non-trivial braiding processes. The key extra ingredient is a generic prescription for constructing string operators. This enables us to derive the existence of anyons with nontrivial braiding statistics based solely on the quantum error correction property.

A. Cleaning lemma

A technical challenge is to construct a pair of open and closed string operators that anti-commute with each other without relying on the macroscopic details of stabilizer generators. The crucial tool is a particular strengthening of the cleaning lemma for 2D local stabilizer codes [25]. Consider square regions A_j of linear size $O(\frac{d}{w})$ which are separated from each other by $O(w)$. Denote the union by $A \equiv \cup_j A_j$, and its complement by $B \equiv A^c$. We will call a subsystem B a *mesh* (Fig.2).

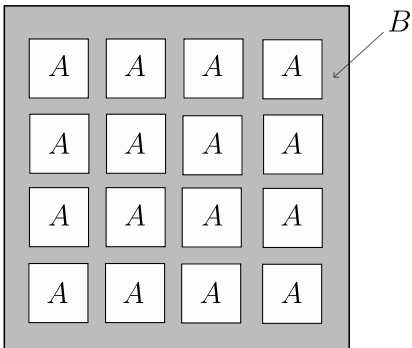


FIG. 2. Each square A_j is correctable and of linear size $O(\frac{d}{w})$. Squares are separated by $O(w)$, so their union A is also correctable. Hence, all the logical operators can be found in the shaded region, a mesh $B = A^c$.

Lemma 3. In a 2D local stabilizer code, no non-trivial logical operator can be supported on A . Equivalently, all logical operators can be supported on a two-dimensional mesh $B = A^c$.

Proof. The lemma was proven in [27], and we will sketch the key arguments. First, note that each square is correctable since the linear size is $O(\frac{d}{w})$. Second, since they are separated by $O(w)$, the union $A = \cup_j A_j$ is also correctable. Finally, due to the cleaning lemma, all the logical operators can be supported on a mesh $B = A^c$. \square

We will use lemma 3 to construct a braiding process. Let ℓ_1, ℓ_2 be a pair of anti-commuting logical operators. Picking a mesh B_1 as in lemma 3, ℓ_1 can be supported on B_1 . We now shift B_1 by $O(w)$ in both horizontal and vertical directions and denote the new mesh by B_2 (Fig. 3). Then, ℓ_2 can be supported on B_2 . Observe that the intersection of ℓ_1 and ℓ_2 is a union of squares of linear size $O(w)$. Since ℓ_1, ℓ_2 anti-commute with each other, they must anti-commute on at least one square. Denote such a square as Q .

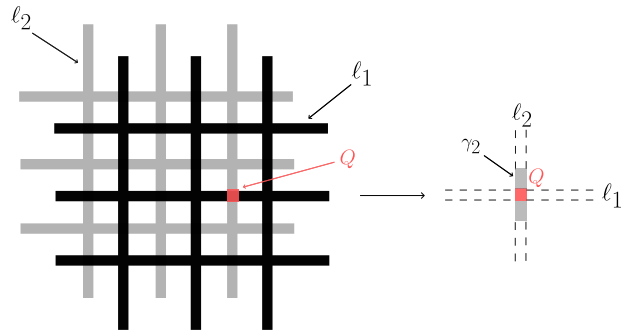


FIG. 3. (Left) A pair of logical operators ℓ_1 and ℓ_2 which anti-commute with each other at one square Q . (Right) A segment of ℓ_2 around Q will be called γ_2 .

B. Braiding process

The goal is to find a braiding process of the form $\gamma_2 \gamma_1 \gamma_2 |\Psi\rangle = -|\Psi\rangle$ where γ_1 is a loop-like stabilizer and γ_2 is a deformable open string operator which anti-commutes with γ_1 . To construct γ_1 , we repeat the above argument for a slightly deformed mesh B'_1 and construct ℓ'_1 , a logical Pauli operator that is equivalent to ℓ_1 and is supported on B'_1 . This is possible as long as the complement of B'_1 consists of squares whose perimeter remains $O(\frac{d}{w})$. Then, $\ell_1 \ell'_1$ is a stabilizer operator supported on $B_1 \cup B'_1$ (Fig. 4).

We will construct a loop-like stabilizer γ_1 from $\ell_1 \ell'_1$ by “truncating” its support away from Q . Namely, for a given region R , let R^+ denote the set of qubits j such that $\text{disc}(j, R) \leq w$.

The following lemma allows us to truncate a large stabilizer S into a smaller stabilizer S' supported on R^+ with possible changes only at the boundary while keeping the operator content on R .

Lemma 4. For any stabilizer operator S and any region R , there exist a stabilizer operator S' , such that (1) $\text{supp}(S') \subseteq R^+$ and (2) $\text{supp}(SS') \cap R = \emptyset$ (equivalently, $S|_{R^c} = S'|_{R^c}$).

Proof. Since S is a stabilizer operator, it can be written as a product of local stabilizer generators $S = \prod_a S_a$.

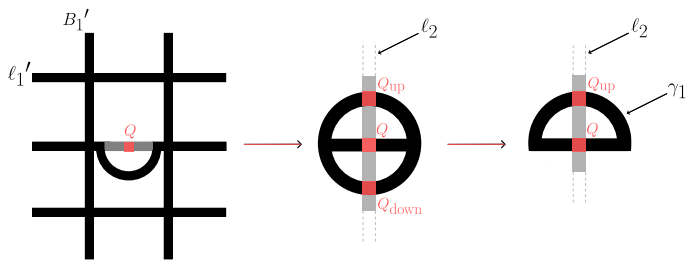


FIG. 4. (Left) An equivalent logical operator ℓ'_1 supported on a deformed mesh B'_1 . (Middle) Starting from a stabilizer operator $S = \ell_1 \ell'_1$ supported on $B_1 \cup B'_1$, we truncate S to obtain a stabilizer operator γ_1 supported around Q . This stabilizer intersects with ℓ_2 at three squares. (Right) We further truncate the stabilizer to obtain γ_1 which intersects with ℓ_2 at two squares.

Specifically, we can decompose S as follows

$$S = \prod_{\text{supp}(S_a) \cap R = \emptyset} S_a \prod_{\text{supp}(S_b) \cap R \neq \emptyset} S_b. \quad (35)$$

Define $S' = \prod_{\text{supp}(S_b) \cap R \neq \emptyset} S_b$. Since the diameter of each S_a is less than w , we know $\text{supp}(S') \subseteq R^+$. Moreover, $\text{supp}(SS') \cap R = \emptyset$ since $SS' = \prod_{\text{supp}(S_a) \cap R = \emptyset} S_a$. \square

The construction of γ_1 proceeds in two steps. First, let us apply the above lemma to truncate $\ell_1 \ell'_1$ into a circular region containing the square Q . The resulting stabilizer operator is supported on a region consisting of a circle and a horizontal line, see the middle panel of Fig. 4 for illustration. Second, we observe that this truncated stabilizer intersects with ℓ_2 at Q_{up} , Q , and Q_{down} . Since this operator anti-commutes with ℓ_2 at Q , it must anti-commute with ℓ_2 at either Q_{up} or Q_{down} . Without loss of generality, we assume that it is Q_{up} . We can then further shrink the stabilizer operator to a semicircular region, as shown in the right panel of Fig. 4, by removing the stabilizer generators below the horizontal line.

This is the desired loop-like stabilizer which we shall use as γ_1 . Note that γ_1 intersects and anti-commutes with ℓ_2 at both Q and Q_{up} .

The construction of γ_2 proceeds in an analogous manner. We start by finding ℓ'_2 in a deformed mesh B'_2 , and then truncate $\ell_2 \ell'_2$ so that it will be supported only near Q_{up} . We can then construct a loop-like stabilizer operator S_2 which intersects and anti-commutes with γ_1 at Q_{up} and Q'_{up} , see Fig. 5 for an illustration. Finally, we decompose S_2 into two segments, $S_2 = \gamma_2 \gamma'_2$, such that γ_2, γ'_2 intersect with γ_1 at Q_{up} and Q'_{up} respectively. We then obtain the desired braiding processes

$$\gamma_2 \gamma_1 \gamma_2 |\Psi\rangle = -|\Psi\rangle, \quad \gamma'_2 \gamma_1 \gamma'_2 |\Psi\rangle = -|\Psi\rangle. \quad (36)$$

C. Overlap with short-range entangled states

The above arguments assume $t = 0$. Applying a finite-depth circuit, the correctable squares now have width

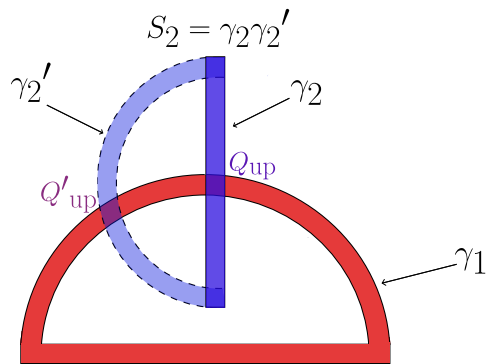


FIG. 5. Braiding process using truncated stabilizer operators.

$\Theta(\frac{d}{w}) - \Theta(t) = \Theta(\frac{d}{w})$, and the separation is now $\Theta(w+t)$. With the braiding processes, the same argument as in lemma 1 implies $|\Psi\rangle \neq U_t |0^n\rangle$ if $\frac{d}{w} > \Theta(w+t)$. We further lower bound $E_t(\Psi)$ using a similar strategy. Starting from a mesh B of width $\Theta(w+t)$, consider a family of meshes, each obtained by shifting the previous meshes along the diagonal by $\Theta(w+t)$. For each pair of meshes, we can repeat the above argument and find an anti-commuting intersection and a local upper bound as in lemma 2. Moreover, each anti-commuting intersection must be separated from each other by $\Theta(w+t)$ and is hence decoupled from each other. The number of such meshes is at least $\Theta(\frac{d}{w(w+t)})$, hence the number of anti-commuting intersections is at least $\Theta(\frac{d^2}{w^2(w+t)^2})$. This completes the proof of theorem 2.

IV. HONEYCOMB MODEL

The original honeycomb model, introduced by Kitaev, is given by [19]

$$H_{\text{Kitaev}} = -J_X \sum_{X\text{-links}} \sigma^x - J_Y \sum_{Y\text{-links}} \sigma^y - J_Z \sum_{Z\text{-links}} \sigma^z \quad (37)$$

where qubits reside on vertices of a honeycomb lattice. The model is exactly solvable via mapping to Majorana fermions. For $J_Z \gg J_X, J_Y > 0$, its low-energy physics can be approximated by the toric code at the leading order in perturbation theory. Hence, from our argument in Section II, we can deduce that the ground state of H_{Kitaev} in the ‘‘toric code phase’’ will satisfy $E_t(\Psi) > O(n)$ for constant t .

Here we will focus on another honeycomb Hamiltonian, denoted as H_{fermion} , that reflects the symmetry properties of the original H_{Kitaev} . The starting point is an observation that the original model H_{Kitaev} possesses pe-

cular loop-like symmetry operators

$$[H_{\text{Kitaev}}, S_{\square}] = 0, \quad S_{\square} = X \begin{array}{c} Y \text{---} Z \\ / \quad \backslash \\ X \quad \quad X \\ \backslash \quad / \\ Z \quad \quad Y \end{array} \quad (38)$$

where S_{\square} can be generated by multiplying all the two-body terms on each hexagon. The ground state $|\Psi_{\text{toric}}\rangle$ of H_{Kitaev} in the toric code phase ($J_Z \gg J_X, J_Y > 0$) satisfies $S_{\square}|\Psi_{\text{toric}}\rangle = |\Psi_{\text{toric}}\rangle$ (i.e. it is vortex-free [19]).

The honeycomb model with emergent fermions, which we shall address in this paper, can be formulated as a 2D stabilizer Hamiltonian

$$H_{\text{fermion}} = - \sum_{\square} S_{\square}, \quad S_{\square} = X \begin{array}{c} Y \text{---} Z \\ / \quad \backslash \\ X \quad \quad X \\ \backslash \quad / \\ Z \quad \quad Y \end{array} \quad (39)$$

where qubits reside on vertices of a hexagonal lattice, and \square are hexagonal plaquettes. A ground state of H_{fermion} satisfies $S_{\square}|\Psi\rangle = |\Psi\rangle$. We will be interested in quantifying the entanglement of wavefunctions that live in the ground space of H_{fermion} .

What are the key differences between H_{Kitaev} and H_{fermion} ? First of all, note that the toric code ground state $|\Psi_{\text{toric}}\rangle$ of H_{Kitaev} is contained in the ground space of H_{fermion} . In fact, the ground space of H_{fermion} is huge. Viewed as a stabilizer code, there are $\frac{n}{2}$ stabilizer generators S_{\square} with one redundancy relation $\prod_{\square} S_{\square} = I$. Hence, the number of logical qubits is $k = 1 + \frac{n}{2}$ which suggests an exponentially large ground state space. Second, as a quantum error-correcting code, H_{fermion} is not fault-tolerant. Indeed, logical operators of the code, which must commute with all S_{\square} , are generated by two-body Pauli operators:

$$X \text{---} X \quad Y \text{---} Y \quad Z \text{---} Z \quad (40)$$

and hence, the code distance is $d = 2$.

Due to an exponential ground state degeneracy and a small code distance, one might think that the honeycomb model has a ground state $|\Psi\rangle$ which would have a large overlap with a short-range entangled state. Contrary to this naive expectation, we will obtain a linear lower bound on $E_t(\Psi)$ for any state $|\Psi\rangle$ in the exponentially large ground space of the honeycomb model.

Theorem 3. Given an arbitrary ground state $|\Psi\rangle$ of the honeycomb model H_{fermion} , there exists $\alpha > 0$ such that of $t \leq O(\sqrt{n})$ we have

$$E_t(\Psi) > \frac{\alpha n}{(t+1)^2}. \quad (41)$$

A. Fermion exchange statistics

A key property of the honeycomb model is that its ground space supports emergent fermions. Consider an

open string operator M which is generated by multiplying two-body logical operators (Eq. (40)). Let us pick an arbitrary ground state $|\Psi\rangle$ and regard it as a ‘‘vacuum’’ state with no fermions. Then, $M|\Psi\rangle$ can be interpreted as a state with two emergent fermions at endpoints of an open string M . A stabilizer generator S_{\square} implements a process of creating and annihilating a pair of fermions, and hence leaving the vacuum state unchanged $S_{\square}|\Psi\rangle = |\Psi\rangle$. These interpretations can be verified by a standard mapping of two-body generators to Majorana fermion operators as in [19].

It is worth emphasizing that a state $M|\Psi\rangle$ with a pair of fermions, as well as the vacuum state $|\Psi\rangle$, live in the ground space of the honeycomb model. This is in contrast with the toric code where anyons emerge as excitations that depart from the ground space of the Hamiltonian.

An immediate challenge is that fermions have trivial braiding statistics (i.e. they are not anyons), and thus the argument from section II is not applicable. In the honeycomb model, this is reflected in that an open string operator M always commutes with a closed string operator S since S is generated by stabilizer generators S_{\square} .

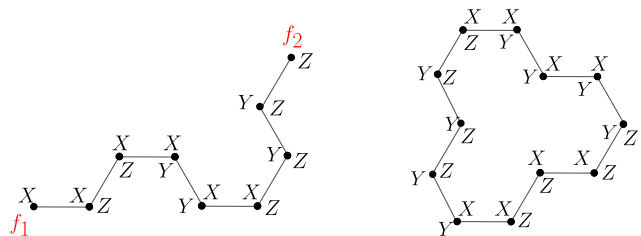


FIG. 6. (Left) An open string operator and (Right) a symmetry operator in the honeycomb model.

Instead, we rely on the fermion exchange statistics to obtain a linear lower bound on $E_t(|\Psi\rangle)$. The topological spin of two fermions can be extracted by the hopping operator algebra due to Levin and Wen [20] which compares the following two pair creation/annihilation processes

$$M_3 M_2 M_1 |\Psi\rangle = e^{i\theta} M_1 M_2 M_3 |\Psi\rangle, \quad (42)$$

where M_i are open string operators as in Fig. 7, and $e^{i\theta} = -1$ for fermions. For the honeycomb model, Eq. (42) can be readily verified as three open string operators M_1, M_2, M_3 with a common endpoint anti-commute with each other. The exchange statistics is stable under deformation by a constant depth circuit U_t by considering dressed string operators and quasi-local fermions.

B. Long-range entanglement

We first prove that a ground state of the honeycomb model is long-range entangled.

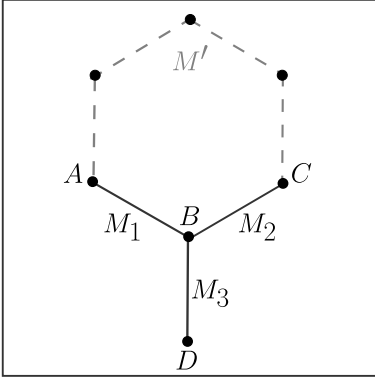


FIG. 7. Exchange statistics of two fermions.

Lemma 5. For any ground state $|\Psi\rangle$ of the honeycomb model, we have

$$U_t|\Psi\rangle \neq |0^n\rangle \quad (43)$$

for any depth- t unitary U_t with constant t .

Proof. Suppose that Eq. (43) is false, namely $|\Psi_t\rangle \equiv U_t|\Psi\rangle = |0^n\rangle$. Let M_1, M_2, M_3 be dressed open string operators satisfying Eq. (42). Using the deformability of string operators, one obtains

$$M_3(M_2M_1)|\Psi_t\rangle = |\psi_{BD}\rangle|\psi_{AC}\rangle|0\rangle^{\otimes(ABCD)^c} \quad (44)$$

where $|\psi_{BD}\rangle, |\psi_{AC}\rangle$ are some wavefunctions supported on BD, AC .

A crucial observation is that $|\psi_{BD}\rangle$ and $|\psi_{AC}\rangle$ are factorized:

$$|\psi_{BD}\rangle|\psi_{AC}\rangle = |\psi_B\rangle|\psi_D\rangle|\psi_A\rangle|\psi_C\rangle. \quad (45)$$

To show this¹, let us construct a deformed string operator M' which connects A and C as in Fig. 7, such that the loop operator $M'M_2M_1$ is a product of some stabilizer generators S_\square , and thus commutes with all string operators. We then have:

$$\begin{aligned} & M_3(M_2M_1)|\Psi\rangle \\ &= M'^\dagger M' M_3(M_2M_1)|\Psi\rangle = M'^\dagger M_3(M'M_2M_1)|\Psi\rangle \\ &= M'^\dagger(M'M_2M_1)M_3|\Psi\rangle = (M_2M_1)M_3|\Psi\rangle \end{aligned} \quad (46)$$

We can, however, write it as $M_2(M_1M_3)|\Psi_t\rangle$ and decompose it as $|\psi_{AD}\rangle|\psi_{BC}\rangle|0\rangle^{\otimes(ABCD)^c}$ similar to Eq. (44), implying:

$$|\psi_{BD}\rangle|\psi_{AC}\rangle = |\psi_{AD}\rangle|\psi_{BC}\rangle. \quad (47)$$

¹ If string operators can be implemented via short-depth circuits (as in the honeycomb model), this statement can be immediately proven. Namely, since the neighborhoods of regions B and D are initially unentangled, B and D cannot be entangled via a short-depth circuit that implements M_3 .

The right-hand side implies B and D are unentangled, and so are A and C . This shows that $|\psi_{BD}\rangle$ and $|\psi_{AC}\rangle$ must be factorized as in Eq. (45).

By properly choosing the phases of $|\psi_B\rangle, |\psi_C\rangle$ and $|\psi_D\rangle$ in order, we can assume

$$\begin{aligned} M_1|\Psi_t\rangle &= |\psi_A\rangle|\psi_B\rangle|0\rangle^{\otimes(AB)^c} \\ M_2M_1|\Psi_t\rangle &= |\psi_A\rangle|\psi_C\rangle|0\rangle^{\otimes(AC)^c} \\ M_3|\Psi_t\rangle &= |\psi_B\rangle|\psi_D\rangle|0\rangle^{\otimes(BD)^c}. \end{aligned} \quad (48)$$

Using the first two equations, we obtain $M_2|\psi_B\rangle|0\rangle^{\otimes(AB)^c} = |\psi_C\rangle|0\rangle^{\otimes(AC)^c}$. Therefore,

$$\begin{aligned} & M_1M_2M_3|\Psi_t\rangle \\ &= M_1M_2|\psi_B\rangle|\psi_D\rangle|0\rangle^{\otimes(BD)^c} = M_1|\psi_C\rangle|\psi_D\rangle|0\rangle^{\otimes(CD)^c} \\ &= |\psi_A\rangle|\psi_B\rangle|\psi_C\rangle|\psi_D\rangle|0\rangle^{\otimes(ABCD)^c} \\ &= M_3(M_2M_1)|\Psi_t\rangle \end{aligned} \quad (49)$$

which contradicts with $e^{i\theta} = -1$. \square

C. Overlap with short-range entangled state

We can prove the following upper bound on the maximum overlap between ρ_R and $|0_R\rangle$.

Lemma 6. Let R to be any patch of linear size $\geq 8(t+1)$. Given any deformed honeycomb model ground state $|\Psi_t\rangle = U_t|\Psi\rangle$ with a depth t circuit U_t , there exists a constant $\epsilon > 0$ such that, in terms of the trace norm,

$$\|\rho_R - |0_R\rangle\langle 0_R|\|_1 > \epsilon, \quad (50)$$

where $\rho_R = \text{Tr}_{R^c}(|\Psi_t\rangle\langle\Psi_t|)$, and accordingly,

$$\mathcal{F}(|0_R\rangle, \rho_R) < 1 - \frac{1}{4}\epsilon^2 = 1 - \epsilon' \quad (51)$$

for some $\epsilon' > 0$.

The proof can be readily obtained by making the proof of lemma 5 more quantitative with each equation replaced with \approx in terms of the trace distance (see appendix Eq. (A) for the full proof). We emphasize that all we need to assume on ρ_R is the deformability of string operators (resulting from 1-form symmetry) and the fermionic exchange statistics (resulting from anomalous nature of symmetry).

Finally, we prove a linear lower bound on $E_t(\Psi)$ for a honeycomb model ground state. Let us divide the whole system into multiple regions R_j with $R = \cup_{j=1}^n R_j$. Unlike the toric code, the honeycomb model does not satisfy the decoupling property as in Eq. (32) since the code distance is small. Instead, we proceed by considering post-projection states sequentially and bound the total projection amplitude.

Let Π_j be an operator that projects \mathcal{H}_{R_j} to $|0_{R_j}\rangle$. Recall that

$$\mathcal{F}(|\Psi_t\rangle, |0^n\rangle) \leq \text{Tr}(\Pi_R \rho_R). \quad (52)$$

We can express the right hand side as (define $\Pi_0 = I$)

$$\text{Tr}(\Pi_R \rho_R) = \prod_{j=1}^m \mathcal{F}_j, \quad \text{where } \mathcal{F}_j \equiv \frac{\text{Tr}(\Pi_j \cdots \Pi_1 \rho_R)}{\text{Tr}(\Pi_{j-1} \cdots \Pi_1 \rho_R)}. \quad (53)$$

We claim that $\mathcal{F}_j < 1 - \epsilon'$ for some $\epsilon' > 0$ and $\forall 1 \leq j \leq m$. To prove this, we define a normalized post-projection state by

$$\rho^{(j)} \equiv \frac{\Pi_j \cdots \Pi_1 \rho_R \Pi_1 \cdots \Pi_j}{\text{Tr}(\Pi_j \cdots \Pi_1 \rho_R)}, \quad (0 \leq j \leq m-1) \quad (54)$$

where $\mathcal{H}_{R_1}, \dots, \mathcal{H}_{R_j}$ have been projected to $|0\rangle$'s. Observe that the normalized post-projection state $\rho^{(j)}$ still satisfies the deformability of the string operators and the fermion exchange statistics inside the patch R_{j+1} , namely

$$\text{Tr}(M_3 M_2 M_1 M_3 M_2 M_1 \rho^{(j)}) = -1 \quad (55)$$

when M_j are supported in R_{j+1} . Therefore, we can apply lemma 6 to $\rho^{(j)}$ and region R_{j+1} to obtain

$$\mathcal{F}_{j+1} = \mathcal{F}(\rho^{(j)}, \Pi_{j+1}) < 1 - \epsilon'. \quad (56)$$

Multiply everything together, we arrive at

$$\mathcal{F}(|\Psi_t\rangle, |0^n\rangle) < (1 - \epsilon')^{\frac{cn}{(t+1)^2}} \quad (57)$$

which proves Thm 3.

D. Mixed state

Quantum circuit complexity of preparing a mixed state has been studied in quantum information theory in the context of topological quantum memory at finite temperature. Recently, there have been renewed interest in classifications of mixed state phases in the condensed matter community. Here, we discuss the implication of our results from the perspective of mixed-state phases.

Following Hastings [21], we say that a mixed state ρ is short-range entangled if ρ can be expressed as a probabilistic ensemble of short-range entangled states:

$$\rho = \sum_j p_j |\psi_j\rangle\langle\psi_j|, \quad |\psi_j\rangle = U_j |0\rangle^n. \quad (58)$$

For a technical reason, it is conventional to assume that the depth of U_j is at most $t \sim O(\text{polylog}(n))$ in defining short-range entanglement in ρ . Previous works showed that two-dimensional commuting projector Hamiltonians and three-dimensional fracton models have short-range entangled Gibbs states according to this definition [21, 28].

We are interested in the quantum circuit complexity of the maximally mixed state ρ that satisfies $\text{Tr}(\rho S_\square) = 1$.

For any decomposition $\rho = \sum_j p_j |\psi_j\rangle\langle\psi_j|$, $\text{Tr}(\rho S_\square) = 1$ and $\|S_\square\| = 1$ would imply

$$S_\square |\psi_j\rangle = 1 \quad (59)$$

for all j . It follows from Theorem 3 that each $|\psi_j\rangle$ is long-range entangled. Hence, we arrive at the following result.

Corollary 1. Any mixed state ρ in the honeycomb model H_{fermion} ground state subspace is long-range entangled.

It is not difficult to extend the above result to the approximate setting.

V. DISCUSSIONS

We will comment on a few open problems.

- 1) Given the recent increasing interest in mixed-state quantum phases, anomalous symmetries and non-invertible symmetries, it will be useful to generalize the notion of depth- t GEM to mixed states. A natural generalization will be to consider the maximum fidelity between the state of interest and an ensemble of short-range entangled states.
- 2) A similar quantitative characterization of entanglement may be obtained for symmetry-protected topological order by considering an overlap with trivial wavefunctions that are prepared by short-depth symmetric circuits (i.e. symmetry-protected GEM).
- 3) The GEM can quantitatively distinguish genuine long-range entanglement from “trivial” long-range entanglement. For instance, we have $E_t(\text{toric}) \sim \Theta(n)$ and $E_t(\text{GHZ}) \sim O(1)$. One potential manifestation of different GEM scaling is (in)stability of long-range entanglement under local decoherence. It will be interesting to make this intuition concrete by establishing a connection between fault tolerance and GEM.
- 4) Studies of depth- t GEM for critical systems (those described by conformal field theories) may also be an interesting research avenue.
- 5) Ground states of a topologically ordered Hamiltonian can be generically prepared by $O(L)$ -depth quantum circuits, and as such, have $E_t(\Psi) \approx 0$ for $t \sim \Omega(L)$. In a system of n qubits, however, there exist quantum states whose preparation requires $e^{O(n)}$ -depth quantum circuits. An example of a quantum state with exponential complexity is a Haar random state. It will be interesting to study the behavior of $E_t(\Psi)$ for states prepared from local random unitary circuits.

ACKNOWLEDGMENTS

We thank Timothy Hsieh, Han Ma, Zi-Wen Liu, and Chong Wang for useful discussions and comments. We especially thank Sergey Bravyi for collaboration on a related work [18] and many illuminating discussions. Research at Perimeter Institute is supported in part by the Government of Canada through the Department of Innovation, Science and Economic Development and by

the Province of Ontario through the Ministry of Colleges and Universities.

Note added: While we are finalizing the manuscript, version 2 of Ref. [22] appeared on arXiv on May 7th 2024. This updated version establishes that a mixed state with anomalous 1-form symmetry exhibits long-range entanglement. Version 1 of Ref. [22], which appeared on arXiv in July 2023, does not contain this result.

-
- [1] A Yu Kitaev, “Fault-tolerant quantum computation by anyons,” *Annals of physics* **303**, 2–30 (2003).
- [2] Eric Dennis, Alexei Kitaev, Andrew Landahl, and John Preskill, “Topological quantum memory,” *Journal of Mathematical Physics* **43**, 4452–4505 (2002).
- [3] Sergey Bravyi, Matthew B Hastings, and Frank Verstraete, “Lieb-robinson bounds and the generation of correlations and topological quantum order,” *Physical review letters* **97**, 050401 (2006).
- [4] Alexei Kitaev and John Preskill, “Topological entanglement entropy,” *Physical review letters* **96**, 110404 (2006).
- [5] Michael Levin and Xiao-Gang Wen, “Detecting topological order in a ground state wave function,” *Physical review letters* **96**, 110405 (2006).
- [6] Bowen Shi, “Verlinde formula from entanglement,” *Physical Review Research* **2**, 023132 (2020).
- [7] Bowen Shi, Kohtaro Kato, and Isaac H Kim, “Fusion rules from entanglement,” *Annals of Physics* **418**, 168164 (2020).
- [8] Isaac H Kim and Benjamin J Brown, “Ground-state entanglement constrains low-energy excitations,” *Physical Review B* **92**, 115139 (2015).
- [9] Michael A Levin and Xiao-Gang Wen, “String-net condensation: A physical mechanism for topological phases,” *Physical Review B* **71**, 045110 (2005).
- [10] Jeongwan Haah, “An invariant of topologically ordered states under local unitary transformations,” *Communications in Mathematical Physics* **342**, 771–801 (2016).
- [11] Dorit Aharonov and Yonathan Touati, “Quantum circuit depth lower bounds for homological codes,” arXiv preprint arXiv:1810.03912 (2018).
- [12] Tzu-Chieh Wei and Paul M Goldbart, “Geometric measure of entanglement and applications to bipartite and multipartite quantum states,” *Physical Review A* **68**, 042307 (2003).
- [13] Alonso Botero and Benni Reznik, “Scaling and universality of multipartite entanglement at criticality,” arXiv preprint arXiv:0708.3391 (2007).
- [14] Román Orús, “Universal geometric entanglement close to quantum phase transitions,” *Physical review letters* **100**, 130502 (2008).
- [15] Román Orús, “Geometric entanglement in a one-dimensional valence-bond solid state,” *Physical Review A* **78**, 062332 (2008).
- [16] Tzu-Chieh Wei, “Entanglement under the renormalization-group transformations on quantum states and in quantum phase transitions,” *Physical Review A* **81**, 062313 (2010).
- [17] Román Orús, Tzu-Chieh Wei, Oliver Buerschaper, and Maarten Van den Nest, “Geometric entanglement in topologically ordered states,” *New Journal of Physics* **16**, 013015 (2014).
- [18] Sergey Bravyi, Dongjin Lee, Zhi Li, and Beni Yoshida, “How much entanglement is needed for quantum error correction?” arXiv preprint arXiv:2405.01332 (2024).
- [19] Alexei Kitaev, “Anyons in an exactly solved model and beyond,” *Annals of Physics* **321**, 2–111 (2006).
- [20] Michael Levin and Xiao-Gang Wen, “Fermions, strings, and gauge fields in lattice spin models,” *Physical Review B* **67**, 245316 (2003).
- [21] Matthew B Hastings, “Topological order at nonzero temperature,” *Physical review letters* **107**, 210501 (2011).
- [22] Zijian Wang, Zhengzhi Wu, and Zhong Wang, “Intrinsic mixed-state topological order without quantum memory,” arXiv preprint arXiv:2307.13758v1 (2023).
- [23] Xie Chen, Zheng-Xin Liu, and Xiao-Gang Wen, “2d symmetry protected topological orders and their protected gapless edge excitations,” in *APS March Meeting Abstracts*, Vol. 2012 (2012) pp. B31–015.
- [24] Leonardo A Lessa, Meng Cheng, and Chong Wang, “Mixed-state quantum anomaly and multipartite entanglement,” arXiv preprint arXiv:2401.17357 (2024).
- [25] Sergey Bravyi and Barbara Terhal, “A no-go theorem for a two-dimensional self-correcting quantum memory based on stabilizer codes,” *New Journal of Physics* **11**, 043029 (2009).
- [26] Sergey Bravyi, Matthew B Hastings, and Spyridon Michalakis, “Topological quantum order: stability under local perturbations,” *Journal of mathematical physics* **51** (2010).
- [27] Sergey Bravyi, David Poulin, and Barbara Terhal, “Tradeoffs for reliable quantum information storage in 2d systems,” *Physical review letters* **104**, 050503 (2010).
- [28] Karthik Siva and Beni Yoshida, “Topological order and memory time in marginally-self-correcting quantum memory,” *Physical Review A* **95**, 032324 (2017).

Appendix A: Proof of lemma 6

Here we prove lemma 6, copied below for convenience.

Lemma 6. Let R to be any patch of linear size $\geq 8(t+1)$. Given any deformed honeycomb model ground state $|\Psi_t\rangle = U_t|\Psi\rangle$ with a depth t circuit U_t , there exists a constant $\epsilon > 0$ such that, in terms of the trace norm,

$$\|\rho_R - |0_R\rangle\langle 0_R|\|_1 > \epsilon, \quad (\text{A1})$$

where $\rho_R = \text{Tr}_{R^c}(|\Psi_t\rangle\langle\Psi_t|)$, and accordingly,

$$\mathcal{F}(|0_R\rangle, \rho_R) < 1 - \frac{1}{4}\epsilon^2 = 1 - \epsilon' \quad (\text{A2})$$

for some $\epsilon' > 0$.

Proof. Similar to the proof of lemma 2, we use \approx to denote closeness in the trace distance

$$\rho \approx \sigma \iff \|\rho - \sigma\|_1 < O(\epsilon). \quad (\text{A3})$$

For pure states, we use two different notions of closeness:

$$\begin{aligned} \psi_1 \approx \psi_2 &\iff \|\psi_1\rangle\langle\psi_1| - |\psi_2\rangle\langle\psi_2|\|_1 < O(\epsilon), \\ |\psi_1\rangle \sim |\psi_2\rangle &\iff \||\psi_1\rangle - |\psi_2\rangle\| < O(\epsilon). \end{aligned} \quad (\text{A4})$$

Here, the norm in the second line is the vector norm in Hilbert space. While \approx ignores the phase information, the approximation \sim cares about the phases. It is clear that $\psi_1 \approx \psi_2$ if and only if we can choose phases so that $\psi_1 \sim \psi_2$.

Now, assuming $\rho_R \approx |0_R\rangle\langle 0_R|$ in a region R , let us derive a contradiction. In the following, M_i are dressed operators, and we omit the subscript t .

First, same as Eq. (27) as its proof, a string operator creates two excitations at endpoints which are approximately decoupled from the rest of the system:

$$M_3 |0_R\rangle \approx |\psi\rangle_{BD} |0\rangle^{\otimes(BD)^c}. \quad (\text{A5})$$

With a similar equation for $M_2 M_1$, we get the approximate version of Eq. (44):

$$\begin{aligned} M_3(M_2 M_1) |0_R\rangle &\approx M_3 |\psi\rangle_{AC} |0\rangle^{\otimes(AC)^c} \\ &\approx |\psi\rangle_{AC} |\psi\rangle_{BD} |0\rangle^{\otimes(ABCD)^c}. \end{aligned} \quad (\text{A6})$$

Here, in the second approximation, we used $M_3(|0\rangle\langle 0|)^{\otimes(AC)^c} M_3^\dagger = \text{Tr}_{AC}(M_3 |0_R\rangle\langle 0_R| M_3^\dagger)$ and Eq. (A5). Also, similarly, we have

$$M_2(M_1 M_3) |0_R\rangle \approx |\psi\rangle_{BC} |\psi\rangle_{AD} |0\rangle^{\otimes(ABCD)^c}. \quad (\text{A7})$$

Then, we show that both $|\phi\rangle_{AC}$ and $|\phi\rangle_{BD}$ approximately factorize. From $\rho_R \approx |0_R\rangle\langle 0_R|$ and $M_3 M_2 M_1 \rho_R = M_2 M_1 M_3 \rho_R$, we get $M_3 M_2 M_1 |0_R\rangle \approx M_2 M_1 M_3 |0_R\rangle$. Now take Tr_{BC} on Eq. (A6) and Eq. (A7) and use the monotonicity of the trace distance under partial trace, we get:

$$\phi_A \otimes \phi_D \approx |\psi\rangle\langle\psi|_{AD}, \quad (\text{A8})$$

where $\phi_A = \text{Tr}_C(|\psi\rangle\langle\psi|_{AC})$ and $\phi_D = \text{Tr}_B(|\psi\rangle\langle\psi|_{BD})$. It follows that ϕ_A and ϕ_D are approximately pure states as measured by the purity²:

$$\text{Tr}((\phi_A \otimes \phi_D)^2) = 1 - O(\epsilon), \quad (\text{A9})$$

which further implies that they are close to pure states in the trace norm³. Therefore, we arrive at the approximate version of Eq. (45).

$$\begin{aligned} M_2 M_1 M_3 |0_R\rangle &\approx M_3 M_2 M_1 |0_R\rangle \\ &\approx |\psi\rangle_A |\psi\rangle_C |\psi\rangle_B |\psi\rangle_D |0\rangle^{\otimes(ABCD)^c}. \end{aligned} \quad (\text{A10})$$

Finally, we can derive a contradiction by considering the phase. The proof is the same as that of lemma 5. We simply replace $=$ by \sim , which keeps the phase information. \square

² For any two states σ_1 and σ_2 , we have $\text{Tr}(\sigma_1^2 - \sigma_2^2) \leq 2\|\sigma_1 - \sigma_2\|_1$.

³ For any σ , denote the eigenvalues as λ_i , then $\lambda_{\max} = \sum_i \lambda_{\max} \lambda_i \geq \sum_i \lambda_i^2 = \text{Tr}(\sigma^2)$. Hence $\|\sigma - P_{\max}\|_1 = 2(1 - \lambda_{\max}) \leq 2(1 - \text{Tr}(\sigma^2))$ where P_{\max} is the projector to the eigenspace corresponding to the largest eigenvalue.